XLI CILAMCE
XLI Ibero-Latin American Congress on Computational Methods in Engineering
16-19 November, 2020 FOZ DO IGUAÇU PARANÁ - BRAZIL

Computational modeling of steel fiber reinforced concrete

Victor Sloboda[1], Roberto Dalledone Machado[1,2], Ricardo Pieralisi[2]

[1]*Programa de Pós Graduação em Métodos Numéricos em Engenharia, Universidade Federal do Paraná*
Av. Cel. Francisco H. dos Santos, 100, 81531-980, Curitiba (PR), Brazil
victorsloboda@hotmail.com, roberto.dalledonemachado@gmail.com
[2]*Programa de Pós Graduação em Engenharia de Construção Civil, Universidade Federal do Paraná*
Av. Cel. Francisco H. dos Santos, 100, 81531-980, Curitiba (PR), Brazil
roberto.dalledonemachado@gmail.com, ricpieralisi@gmail.com

Abstract. New building technologies are developed with the goal of improving structural performance. One very promising technology is the steel fiber reinforced concrete (SFRC), in which steel fibers are added in the concrete mixture. Concrete is a fragile material whose tensile resistance is very lower than compressive. Steel reinforcement, as well as steel fibers, improves the tensile behavior, grants more ductility to concrete and increases cracking and spalling resistance. Although SFRC is considered promising, there are still a few reliable computational models to analyze and predict the behavior of SFRC. The modeling is difficult because of the random distribution of fibers and the consequent anisotropy. A numerical and computational approaching, using numerical methods, is used to develop this work. Different constitutive models are analyzed and the results are compared with experimental data obtained from flexural tests. This work aims to extend the application of the SFRC in various situations, for example the precast structures.

Keywords: Concrete. Steel fiber. Modeling. Cracking.

1 Introduction

The idea of adding fibers in a material dates back to the ancient Egypt. The steel fiber reinforced concrete was invented about 1960 and 1970 (Bentur and Mindess [1]). Concrete, most used material in civil construction (Figueiredo [2]), is a versatile and low-cost material (Mehta et al. [3]; Marchetti and Botelho [4]), however, it is brittle and has low tensile strenght. Due to this shortcoming, steel bars, a material with high tensile strenght, are added, resulting in reinforced concrete. However, the cross sections of reinforced concrete are quite heterogeneous, whose zones of greatest tensile resistance are located in steel bar reinforcement. Fibers, unlike steel bars, distribute the tensile stresses across the cross section of the structure (Kosmatka et al. [5]), and can save the need of a frame sector at the construction worksite.

The goal of this work is to analyze how the addition of steel fibers can improve the behavior of concrete. This performance improvement is observed by modeling tests made in concrete structures, obtained with computational programs and numerical methods, mainly the Finite Element Method (FEM). After that, the results are compared with information from the literature or results recommended by the regulations.

The occurrence of catastrophic incidents, broadcast by midia, involving the collapse of concrete structures, is one of the main reasons for choosing the addressed topic. Several critical incidents could be avoided or mitigated if the quality of the collapsed structures was better. The fibers can help slow the crack growth or propagation process and grant more ductility to the concrete, since the collapse is fragile and sudden.

Furthermore, cementitious materials with fibers are still underused, due mainly to the high cost and the decreasing in the workability of the mixture. Another reason is the relative insipience of this technology, mainly in Brazil, where research data on fiber reinforced concrete, as well as specific norms, is still lacking (Figueiredo [2]). Finally, the current constitutive models of the SFRC are not able to faithfully simulating the properties of the composite, due to the random distribution of the fibers (Bitencourt Jr et al. [6]).

2 Revision

2.1 Materials

The SFRC is a composite material (concrete matrix and the steel fibers) (Jones [7]).

Concrete is a heterogeneous material with two phases: cement matrix and aggregates. One of its limitations is the great difference between tension and compression behaviors. Another limitation is the fragility, mainly under tensile stresses. Thus, reinforced concrete has complemmentary tensile resistance and additional ductility, given by steel bars or fibers (Bitencourt Jr et al. [6]).

The distribution of fibers in the concrete mixture is random, but the direction of casting intervenes considerably on distribution. Because of this, the fiber reinforced concrete is anisotropic.

There are various types of fibers: vegetal, polimeric, carbon, glass, steel, among others (HERSCOVICI et al. [8]; PASA [9]). Steel fibers can take various shapes, surfaces and cross-sections.

2.2 SFRC Performance

According to Model Code CEB-FIp 2010 (FIB [10]), the main advantage of the fiber is to guarantee tensile resistance after cracking starts, in addition to increasing the tensile strenght. The fibers modify the stress-strain diagram mainly after the peak; in other words, they act after the beginning of cracking. They do not prevent nor delay the cracking, but lessen its effects. In addition, Fig. 1 shows how fibers reduce the stress concentration at the end of a crack.

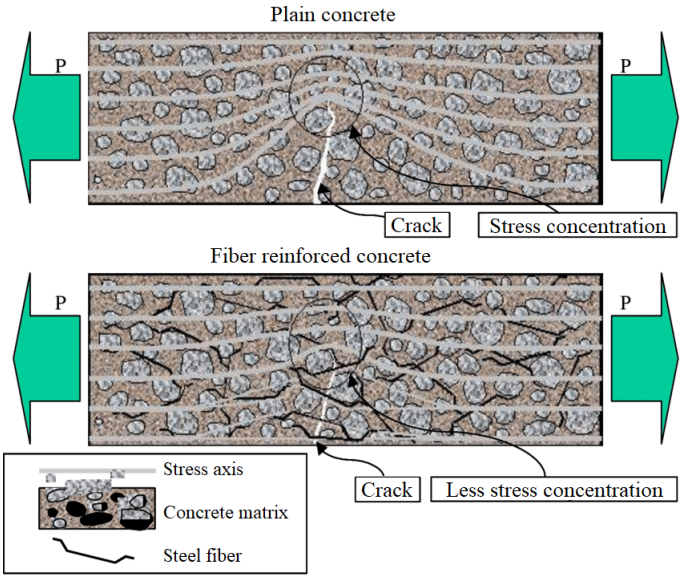

Figure 1. Stress concentration decreasing due to fibers (adapted from Figueiredo [2])

Some fiber attributes must be considered:

- Shape: wavy or hooked fibers grant more pullout resistance than straight fibers.
- Surface: rough fibers grant better grip than plain fibers, due to greater contact surface to the matrix.
- Content: as more fibers, more resistance. However, the cost increases and the workability is impaired.
- Cross section: as greater the area, greater the strenght; as greater the perimeter, better the grip (more contact area between the fiber and the matrix).
- Lenght: longer fibers are better, but not as long, otherwise they break more easily. Too short fibers have low pullout resistance (Figueiredo [2]).
- Aspect ratio: the bigger, the more strenght (Singh [11]).

Remark 1: Compression. The stress-strain diagram for compression before the peak (pre-crack) undergoes little changing with the addition of fibers, because the latter act when the cracking begins. In Fig. 2, the curves for conventional concrete and fiber reinforced concrete pratically coincide until the peak. After the peak, the area

under the curve is greater for the fiber reinforced concrete (more strenght). There is not a vertical extension (does not increase in compressive resistance), but a horizontal extension (post-cracking ductility). The fibers decrease the width of cracks and favor the branching of cracks, instead a straight propagation (Kosmatka et al. [5]).

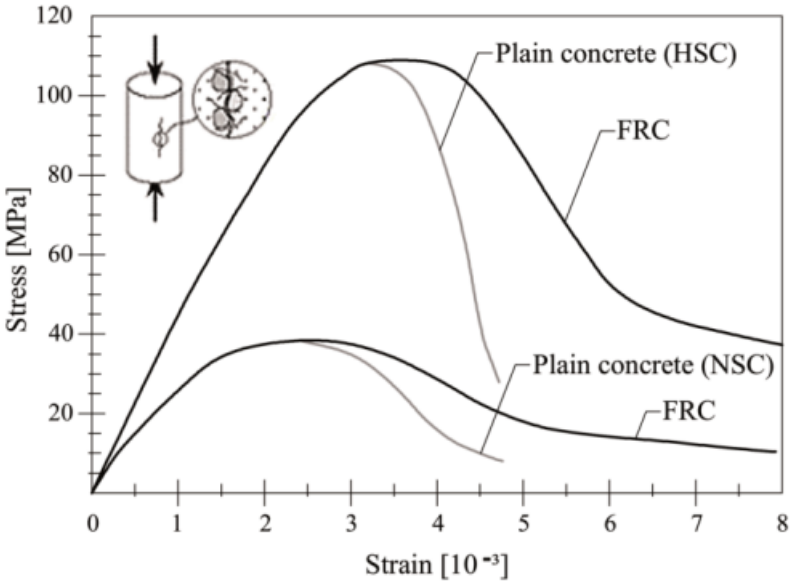

Figure 2. Comparation between conventional concrete and fiber reinforced concrete under compression (adapted from FIB [10])

Remark 2: Tension. The concrete begins to crack at low tensile stresses. The steel fiber behaves just as the steel reinforcement bar. Since the steel resists highly to tensile stresses and is ductile, the combination of concrete and steel fiber modifies the stress-strain diagram. The peak stress increases, so there is an addition of tensile strenght compared to the plain concrete. If the fiber content is less than the critical content (Figueiredo [2]), the strain softening behavior occurs after cracking. If the fiber content is greater than the critical content, the strain hardening is observed.

Remark 3: Bending. Before cracking, the flexural behavior is linear-elastic. When the first crack opens, stresses rearrange themselves and the neutral axis moves toward the most compressed edge (generally the top edge). The stress distribution is no longer linear, differently of the strain distribution, though.

Remark 4: Cracking. The cracks are initially small, but they increase with time and loading. Due to stress concentration, a plasticity flow may occur provoking loss of energy, dissipated by the cracks. As the structure cracks, the loading capacity and stiffness decrease – this highlights the non-linearity of the concrete. The cracking growth is observed with the increasing crack width, number or spread of the crack, among other effects. When a concrete structure is critically cracked, it suddenly collapses, due to the fragility. There are several factors that favor the collapse, for instance, the discontinuities at the cement paste, the empty spaces and the break of the interface mortar-aggregate (Kotsovos [12]).

2.3 Finite Element Method (FEM)

This work uses the Finite Element Method (FEM), in which the structure is discretized in smaller elements interconnected by nodes. The boundary conditions and external links are applied (respectively, supports and loads). The more elements (e.g., the more refined the mesh of finite elements), the closer the model results converge to analytical solution (Soriano and Lima [13]).

To proceed with FEM, it is necessary to define shape functions. The chosen shape functions are Lagrange quadratic polynomials.

To observe the behavior of a structure, it is necessary to know the constitutive law of the material. The

hypotesis of stress plain state was adopted. The matrix of constitutive relations D is (ν is Poisson ratio and E is the Young modulus):

$$[D] = \frac{E}{1-\nu^2}\begin{bmatrix} 1 & \nu & 0 \\ \nu & 1 & 0 \\ 0 & 0 & \frac{1-\nu}{2} \end{bmatrix}. \tag{1}$$

2.4 Mathematic formulation

The elementar stiffness matrix $[K]^e$ is calculated for each finite element (Soriano and Lima [13]; Oñate [14]):

$$[K]^e = \int_V [B]^T [D][B] dV. \tag{2}$$

The only external force is the load applied at the middle of the beam span.

As the elementary stiffness matrices are calculated, the stiffness coefficients are located at the global stiffness matrix. This rearrangement results in the coupling of the elements. Imposed the boundary conditions, the calculation proceeds with Hooke's law.

In this work, the element used is the nine-nodes isoparametric rectangular element. The shape functions are obtained by Lagrange polynomials.

The matrix $[B]$ contains the derivatives of the shape functions. Because the element is isoparametric, it is necessary to obtain the Jacobian determinant $[J]$ to associate global (x and y) coordinates with isoparametric coordinates (ξ and η).

At stress plain state, thickness t is constant; therefore, the integration is done in the element area.

$$[K]^e = t \int_{-1}^{1} \int_{-1}^{1} [B]^T [D][B]|J| d\xi d\eta. \tag{3}$$

The integral in eq. (3) is calculated by numeric integration (Oñate [14]). This method consists in calculate the sum of values of a function in certain points, obtained by the Gaussian quadrature method. Adapting eq. (3) for numeric integration:

$$[K]^e = t \sum_{i=1}^{n} \sum_{j=1}^{n} \Big[[B(\xi_i, \eta_j)]^T [D][B(\xi_i, \eta_j)]|J| W_i W_j \Big]. \tag{4}$$

Remark 5: Iterative methods for nonlinear equations solving. According to Bathe [15], this is how a nonlinear system of equations is solved:

$$[K(u)]\{u\} = \{r\} - \{f\}. \tag{5}$$

In eq. (5), $[K(u)]$ is the nonlinear stiffness matrix, $\{u\}$ is the displacement vector, $\{r\}$ and $\{f\}$ are, respectively, external and internal force vectors. In nonlinear analysis, as the iterations are processed, the internal forces converge to the external loading and the displacement increment approaches zero.

There are methods to solve nonlinear equations, for instance, full Newton-Raphson and modified Newton-Raphson method (Kotsovos [12]); the latter was chosen, as it requires less computational effort, since the stiffness matrix does not change with iterations, only with load steps.

At each iteration, the global displacement vector receives the displacement increment obtained by eq. (5). For the iteration $i > 0$ and the load step $j > 0$ (Bathe [15]):

$$K_{(i-1)}^{(j-1)} \Delta u_{(i)} = r^{(j)} - f_{(i)}^{(j-1)} \tag{6}$$

$$u_{(i)}^{(j)} = u_{(i-1)}^{(j)} + \Delta u_{(i)}. \tag{7}$$

Like the stiffness matrix in modified Newton-Raphson method, the vector of external forces only vary with the load steps. In addition, the following initial conditions are the absence of displacements and internal forces at the beginning of a load step. When the difference between external and internal forces is less than the chosen tolerance, the next loading step is processed.

Remark 6: Mechanics of damage. The linear behavior of a concrete structure is observed until the cracking begins. Thereafter, the structure's stiffness decreases and the matrix $[K]$ reorganizes to become compatible with the damaged structure. A function must be used to associate the constitutive law of the material with the damage. Despite the SFRC is an anisotropic material, without loss of generality, one consider as an isotropic one. A damaged element is under apparent stress σ, but corresponding to effective stress $\tilde{\sigma}$, given by eq. (8). The relative damage D ranges from zero (fully integer element) to one (fully damaged element). The damage model of Mazars was chosen to simulate the progression of damage of the structure.

$$\frac{\sigma}{\tilde{\sigma}} = 1 - D. \tag{8}$$

2.5 Computational modeling

In this work, a finite element program was developed in the Python language. The analyzed model is a concrete beam 55 cm wide (50 cm span) and square cross section 15x15 cm, made of SFRC, without steel bars (the fibers are the only reinforcement). These dimensions are recommended by EN 14651 [16]. The beam is isostatic and three are displacements restricted (two vertical and one horizontal support). The loading is concentrated and monotonic in the middle of the span, whose step is 1 kN. The chosen element is the 9-node Lagrangean, rectangular and isoparametric element. The roughest mesh has 132 elements and 585 nodes.

The geometry and loading configuration are shown at Fig. 3.

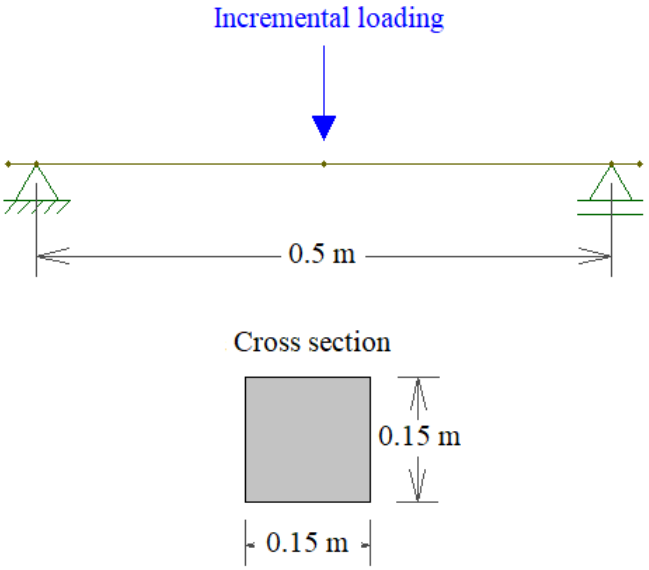

Figure 3. Comparation between conventional concrete and fiber reinforced concrete under compression (own autorship)

The adopted Young modulus was 25 GPa and the Poisson ratio was adopted 0,2. The limit compressive stress adopted was 20 MPa, and the limit tensile stress was obtained by the eq. (9) according to NBR-6118:2014:

$$f_{ctm} = 0.3[f_{ck}]^{\frac{2}{3}}. \tag{9}$$

In eq. (9), f_{ck} is the concrete compressive resistance in MPa and f_{ctm} is the tensile resistance, also in MPa. For $f_{ck} = 20$ MPa, a $f_{ctm} = 2.21$ MPa was obtained.

3 Conclusions

As the program is still under development, the partial results obtained are showed.

First, at Fig. 4, a load-displacement diagram is showed for a loading up to 60 kN, with increments of 1 kN, for a mesh with 528 elements. The final displacement is approximatedly 0.4 mm, a value still below to already obtained results.

Then, at Fig. 5, a map of damage for the mesh (with 528 elements) is showed. The black regions are undamaged zones ($D = 0$). Purple regions are slightly damaged. Medium damage is representated by shades of red and orange. Pale yellow zones are most damaged, whose damage D approaches one.

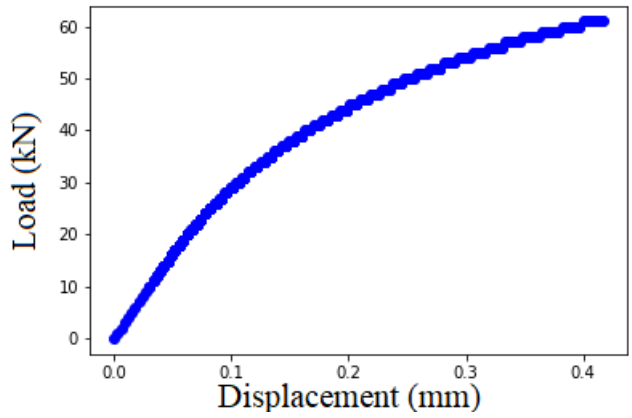

Figure 4. Load-displacement diagram for a mesh with 528 elements (own autorship)

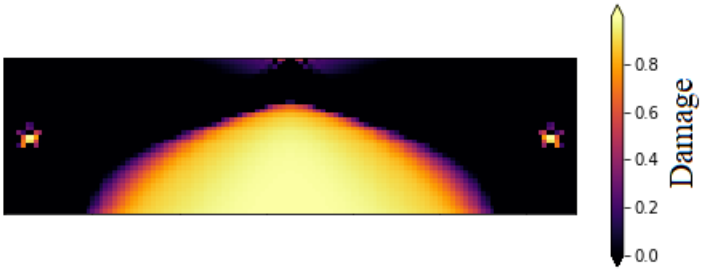

Figure 5. Damaged configuration of the mesh with 528 elements (own autorship)

Authorship statement. The authors hereby confirm that they are the sole liable persons responsible for the authorship of this work, and that all material that has been herein included as part of the present paper is either the property (and authorship) of the authors, or has the permission of the owners to be included here.

References

[1] Bentur, A. & Mindess, S., 2006. *Fibre reinforced cementitious composites*. Crc Press.
[2] Figueiredo, A. D. d., 2011. *Concreto reforçado com fibras.* PhD thesis, Universidade de São Paulo.
[3] Mehta, P. K., Monteiro, P. J., & Carmona Filho, A., 1994. *Concreto: estrutura, propriedades e materiais*. Pini.
[4] Marchetti, O. & Botelho, M. H. C., 2015. *Concreto armado-Eu te amo*, volume 1. Editora Blucher.
[5] Kosmatka, S. H., Kerkhoff, B., Panarese, W. C., et al., 2002. *Design and control of concrete mixtures*, volume 5420. Portland Cement Association Skokie, IL.
[6] Bitencourt Jr, L. A., Manzoli, O. L., Bittencourt, T. N., & Vecchio, F. J., 2019. Numerical modeling of steel fiber reinforced concrete with a discrete and explicit representation of steel fibers. *International Journal of Solids and Structures*, vol. 159, pp. 171–190.
[7] Jones, R. M., 1998. *Mechanics of composite materials*. CRC press.
[8] HERSCOVICI, H., ROEHL, D., & SÁNCHEZ FILHO, E. d. S., 2019. Estudo experimental de vigas curtas de concreto com fibras de aço sujeitas à flexão. *Revista IBRACON de Estruturas e Materiais*, vol. 12, n. 2, pp. 288–307.
[9] PASA, V., 2007. *Análise do comportamento de estruturas de concreto reforçado com fibras de aço via método dos elementos finitos*. PhD thesis, Dissertação (Mestrado em Engenharia de Estruturas), Universidade Federal do Rio Grande do Sul.
[10] FIB, 2013. Fib model code for concrete structures 2010.
[11] Singh, H., 2016. *Steel fiber reinforced concrete: behavior, modelling and design*. Springer.
[12] Kotsovos, M. D., 2015. *Finite-element modelling of structural concrete: short-term static and dynamic loading conditions*. CRC Press.
[13] Soriano, H. L. & Lima, S. d. S., 2003. *Método de Elementos Finitos em Análise de Estruturas Vol. 48*. EdUSP.
[14] Oñate, E., 2009. *Structural analysis with the finite element method. Linear statics: volume 1: basis and solids*. Springer Science & Business Media.
[15] Bathe, K.-J., 2006. *Finite element procedures*. Klaus-Jurgen Bathe.
[16] EN 14651, B. S. B., 2005. A1: 2007, test method for metallic fibre concrete—measuring the flexural tensile strength (limit of proportionality (lop), residual). *British Standard Institute, UK*.